Solar-Terrestrial Physics. 2025, vol. 11, iss. 2, pp. 48–59. DOI: 10.12737/stp-112202505. © 2025
D.D. Pozdnyakova, V.A. Pilipenko, M. Nose, S.Yu. Khomutov, D.G. Baishev. Published by INFRA-M Academic Publishing House

DOI: 10.12737/stp-112202505

Received December 11, 2024
Accepted March 03, 2025

SATELLITE AND GROUND-BASED OBSERVATIONS OF Pc1 PULSATIONS DURING A MAGNETIC STORM IN MARCH 2023

D.D. Pozdnyakova
Schmidt Institute of Physics of the Earth RAS, Moscow, Russia, d_pozdnyakova@live.ru
Institute of Solar-Terrestrial Physics SB RAS, Irkutsk, Russia

V.A. Pilipenko
Schmidt Institute of Physics of the Earth RAS, Moscow, Russia, pilipenko_va@mail.ru

M. Nose
Nagoya City University, Nagoya, Japan, nose.masahito@gmail.com

S.Yu. Khomutov
Institute of Cosmophysical Researches and Radio Wave Propagation FEB RAS, Paratunka, Russia, khomutov@ikir.ru

D.G. Baishev
Yu.G. Shafer Institute of Cosmophysical Research and Aeronomy SB RAS, Yakutsk, Russia, baishev@ikfia.ysn.ru

Abstract. We have analyzed electromagnetic ion-cyclotron oscillations of the Pc1 range (~1 Hz) recorded during the recovery phase of the March 25, 2023 magnetic storm at the network of ground stations in the Far East and at low-orbit SWARM satellites passing over the stations. The collected data made it possible to trace propagation of Pc1 waves through the ionosphere to Earth's surface and along the ionosphere. While long-term (~1 hour) narrowband pulsations were observed at ground stations, satellites recorded only a short (~40 s) burst of transverse oscillations. Estimated coherence of signals between close SWARM-A and -C satellites, separated by ~1° longitude, gives a transverse scale of the wave packet in the ionosphere equal to ~90 km. The long duration of pulsations at ground stations is caused by waveguide propagation of signals along the ionosphere due to which the station "collects" signals from a large magnetospheric region. The presence of waveguide propagation is confirmed by the orientation of the polarization ellipse of ground-based Pc1 pulsations relative to the site of injection of waves into the ionosphere. It is hypothesized that ion-cyclotron instability develops in the form of localized and short-lived bursts, but the mechanism of such a regime remains unclear.

Keywords: Pc1 pulsations, electromagnetic ion-cyclotron waves, SWARM satellites.

INTRODUCTION

Electromagnetic ion cyclotron (EMIC) waves in the Pc1 range of geomagnetic pulsations (from fractions of Hz to a few Hz) have been observed with ground and satellite magnetometers over the decades. The fundamental issues concerning their physical nature and generation mechanism are considered settled: EMIC waves are generated near the equatorial plane of the magnetosphere due to resonant interaction with ring current protons having an energy 10–100 keV [Horne, Thorne, 1994; Gary et al., 1995]. If we assume a bi-Maxwellian energy distribution of energetic protons with parallel $T_{\|}$ and perpendicular $T_{\perp}$ temperatures, kinetic EMIC instability develops under positive anisotropy $A=T_{\perp}/T_{\|}-1>0$. Waves with a finite proton frequency-to-gyrofrequency ratio $\omega/\Omega\leq 1$ having a left-handed circular polarization in the region of the normal Doppler effect (in a fixed reference, waves and particles move toward each other) will be unstable. Anisotropy $A>0$ necessary for the development of the instability occurs either when protons are injected deep into the magnetosphere with subsequent betatron acceleration [Kangas et al., 1998], or when the magnetosphere is compressed by solar wind dynamic pressure pulses [Engebretson et al., 2002; Usanova et al., 2008]. The increment of EMIC-wave growth becomes noticeable under the condition $u_i \gg V_A$, where u_i is the ion thermal velocity, V_A is the Alfvén velocity, i.e. with sufficiently dense background plasma [Arcimovich, Sagdeev, 1979]. Thus, favorable conditions for developing this instability arise either inside the plasmasphere, where the concentration of cold plasma is high [Hu, Fraser, 1994], or outside the geosynchronous orbit, where the magnetospheric magnetic field is low [Hansen et al., 1992]. Satellite studies suggest that Pc1 pulsations do occur both in the outer magnetosphere ($L>7$) during the daytime and in the inner magnetosphere ($L<4$) in the evening [Anderson et al., 1992; Keika et al., 2013].

Observations show that EMIC instability can develop in different modes, and the mechanisms of formation of such modes remain unclear [Trakhtengerts, Rycroft, 2011]. It is generally believed that EMIC instability of ring current protons is convective, i.e. the instability region at the top of the field line acts as an amplifier of traveling EMIC waves [Horne, Thorne, 1993]. The wave packets themselves oscillate between reflective conjugate ionospheres and experience enhancement each time they pass through the equatorial region of the magnetosphere (the Bouncing Wave Packet (BWP) model) [Guglielmi, 1979]. This model is designed to

explain the specific type of Pc1 pulsations — "pearls", which are a regular sequence of wave packets that alternately appear at geomagnetically conjugate points. Nonetheless, this model is becoming increasingly questionable [Mursula et al., 2007]; in particular, there is no model-predicted doubling of the frequency of occurrence of EMIC wave packets in a geostationary satellite as compared to the conjugate ground station [Usanova et al., 2008]. The pearl generator can be EMIC instability in the mode of backward wave oscillator [Trakhtengerts, Demekhov, 2007]. The positive feedback in this mode occurs due to the interaction of an EMIC wave with a modulated beam of particles. At the same time, depending on the beam density, this absolute instability can exist both in the continuous generation regime and in the periodic regime [Demekhov, 2007].

Most Pc1 pulsations are observed as continuous narrowband emission, i.e. they are generated by absolute instability. In a multicomponent plasma with an admixture of heavy ions (He^+, O^+) in the region where the wave frequency is equal to the crossover frequency, polarization inversion, wave partial reflection and absorption can occur [Rauch, Roux, 1982; Johnson, Cheng, 1999; Mikhailova et al., 2012]. With a sufficiently high concentration of heavy ions, EMIC waves can even be trapped near the equatorial plane of the magnetosphere [Guglielmi et al., 2000]. In the Pc1 frequency range, so-called ion-ion hybrid modes propagating across magnetic shells are also recorded in the magnetosphere [Mikhailova et al., 2022]. As a result, in the multicomponent plasma EMIC waves can be trapped not only along the field line, but also across it, in the region with a local minimum of the radial profile of the Alfvén velocity [Mikhailova et al., 2014].

Upon generation, EMIC waves propagate along magnetic field lines, reaching the ionosphere and eventually Earth's surface. As the ionosphere is approached, the ω/Ω ratio becomes so small that the Pc1 waves incident on the ionosphere can be considered magnetohydrodynamic (MHD) modes. Inside the ionosphere, the EMIC wave is partially transformed into a fast magnetosonic (FMS) mode, which can be transported along the ionospheric waveguide at distances up to 1000 km from the injection site of the wave into the ionosphere [Kim et al., 2010]. Thus, the ionosphere acts as a large receiving antenna that collects magnetospheric EMIC signals from a large area at one station. When Pc1 pulsations propagate through the waveguide, their spectral composition at remote stations is cut off from below at the cutoff frequency — the critical frequency of the ionospheric waveguide. Modeling the interaction of EMIC waves with the ionosphere predicts that in the source region the ground response should be predominantly formed by the field of an Alfvén wave incident from the magnetosphere along field lines [Fujita, Tamao, 1988]. At larger distances, the wave field should be caused mainly by the FMS wave propagating along the ionospheric waveguide. As a result, polarization of Pc1 oscillations in the horizontal plane at different distances from the point where the wave is incident on the ionosphere should differ [Fedorov et al., 2018]. In general, the properties of Pc1 waves on Earth are determined by processes of generation in the near-equatorial plane of the magnetosphere, propagation through magnetospheric plasma along field lines to the upper ionosphere, ionospheric propagation, and passage through the ionosphere to Earth.

We have tried to trace and analyze propagation of Pc1 waves through and along the ionosphere, using data from low-orbit satellites and a network of ground stations.

GROUND AND SATELLITE OBSERVATIONS

We have analyzed data from a network of three-component induction magnetometers located in the Far East and Japan at ~20°–56° N. Most of these stations are part of the PWING project (Nagoya University) [Shiokawa et al., 2017]. Geographic and geomagnetic coordinates of the stations are given in Table; the map of the stations is shown in Figure 1. The horizontal components B_x and B_y are oriented in S-N and W-E directions respectively. Since each station has its own frequency response and sensitivity, we cannot directly compare amplitudes at different stations; therefore, we compare waveforms, spectral composition, and polarization of oscillations. However, since we deal with narrowband pulsations at a central frequency of ~ 1 Hz, the amplitude can be approximately estimated by introducing conversion rates from V to nT at the frequency of 1 Hz [https://stdb2.isee.nagoya-u.ac.jp/magne/magne_stations.html]. The rates are listed in a separate column of Table.

For the recorded wave events, SWARM satellites' orbits passed over the network of stations [https://www.esa.int/Applications/Observing_the_Earth/FutureEO/Swarm]. Three identical SWARM satellites A, B, C operate in an almost circular circumpolar (87.3° inclination) orbit in the following configuration: SWARM A and C fly side by side with a longitude difference of ~1° at a height of 460 km; Satellite B, at 530 km. SWARM

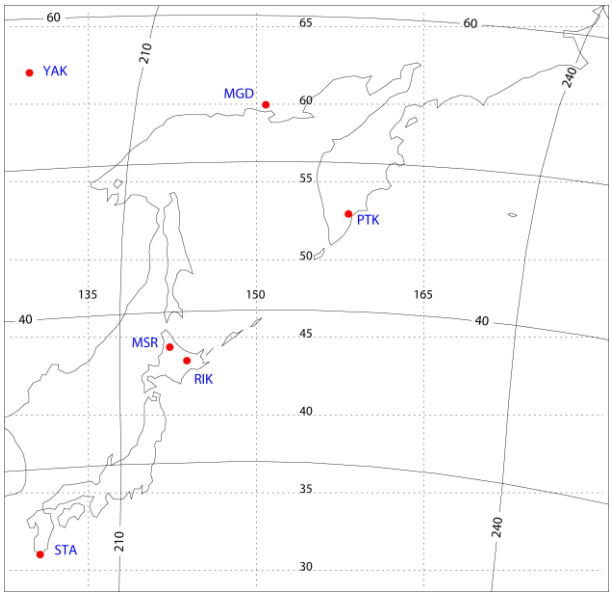

Figure 1. Position of PWING stations. The grid of geographic and geomagnetic coordinates is shown by dotted and solid lines

Information on ground stations

Station	Code	Latitude	Longitude	Geomagnetic latitude	Geomagnetic longitude	Institute	Sensitivity at 1 Hz frequency, V/nT
Yakutsk	YAK	62.02	129.72	56.2	200.5	SHICRA	H, D: 0.19376
Magadan	MGD	60.05	150.73	51.9	213.2	IKIR	H: 0.247 D: 0.253
Paratunka	PTK	52.97	158.28	45.8	221.4	IKIR	H: 0.243 D: 0.246
Moshiri	MSR	44.37	142.27	35.6	209.5	ISEE	H: 10.279 D: 10.501
Rikubetsu	RIK	43.46	143.77	34.7	210.8	ISEE	H, D: 0.459
Sata	STA	31.02	130.68	21.2	200.5	ISEE	H: 0.161 D: 0.163

satellites are equipped with a three-component Vector Field Magnetometer (VFM) with a sampling rate of 50 Hz, a Langmuir probe for measuring plasma density (sampling frequency of 2 Hz), and other instruments. Initial magnetometer data is given in the NEC (North–East–Center) coordinate system: the *N* and *E* components lie in the horizontal plane, pointing to the north and east respectively; *C*, to the center of Earth.

The magnetometer data was converted to the Mean Field-Aligned (MFA) coordinate system, oriented along the current geomagnetic field $\mathbf{B}_0$, which is directed from the Southern Hemisphere to the Northern Hemisphere. As a result, the disturbance field is divided into the field-aligned component B_z, which coincides with $\mathbf{B}_0$, and transverse components $\mathbf{B}_\perp=\{B_x, B_y\}$: the Y-axis is perpendicular to the magnetic meridian and eastward, the X-axis is orthogonal to Z and Y. To compare ground and satellite data, using the Satellite Situation Center resource (NASA) [https://sscweb.gsfc.nasa.gov], we have constructed a projection of orbits of all SWARM satellites along the field line onto the ionosphere (at an altitude of 100 km) for the time intervals considered.

THE MARCH 23–25, 2023 STORM

A strong magnetic storm began on March 23, 2023. During the main phase, the *SYM-H* index was as high as –170 nT. Distinct Pc1 wave packets were observed only during the recovery phase on March 25, 2023 at middle- and low-latitude stations. Pc1 pulsations in two intervals have been selected for detailed analysis.

Interval A. Long-term narrowband (~1 Hz) pulsations at ground stations occurred at night at 11:40–12:40 UT (~21 LT for Japanese stations and around midnight for Kamchatka). Figure 2 displays spectrograms (B_x) from the chain of stations according to decreasing latitude: YAK, PTK, MSR, RIK, STA. The signal at RIK is complicated by high-frequency interference.

Interval B. At 14:15–14:45 UT (~23:30 LT for Japanese stations, and ~02:30 LT for Kamchatka), there was the most pronounced series of Pc1 pulsations. The B_x spectrograms (Figure 3) show the presence of narrowband pulsations with a central frequency of ~1.3 Hz at both subauroral stations (MGD, YAK) and the low-latitude stations (PTK, MSR, RIK, STA).

For each interval, we have drawn a map of the stations and the geomagnetic projection of the orbit of each SWARM satellite along the field line onto the lower ionosphere (100 km) (Figure 4). In interval A, SWARM A and C passed over the stations; and in interval B, SWARM B. The Pc1 burst in the ionosphere was recorded when the satellite's orbit projection was at a geomagnetic latitude of ~50° between YAK and MSR.

SYNCHRONOUS SATELLITE AND GROUND OBSERVATIONS OF Pc1 PACKETS

Pc1 oscillations were recorded by SWARM A and C at the same frequency as ground Pc1 pulsations. In the analyzed intervals, SWARM A and C flied over the stations of the latitudinal profile from the Southern Hemisphere to the Northern Hemisphere. We compared the B_x spectrogram from YAK with the spectrogram from the SWARM satellite (B_y in the MFA coordinate system) for intervals A (Figure 5) and B (Figure 6).

To represent the position of the proposed source of Pc1 pulsations relative to the plasmapause, we have plotted variations in plasma density N_e, using SWARM data (top panel in Figures 5, 6). The observed deep trough in N_e — the so-called plasma trough — corresponds to the ionospheric projection of the plasmapause. In interval A, the satellite entered the plasma trough at ~11:48 UT; and in interval B, at ~14:17 UT. Thus, in both intervals the Pc1 signal was detected inside the plasmasphere near the plasmapause.

LATITUDINAL STRUCTURE OF THE Pc1 PULSATION FIELD

To examine in more detail the change in spectral composition as it propagates, we have obtained normalized signal spectra of all stations according to the B_x component for intervals A and B (Figure 7, *a*, *b*). In interval A, the spectral maximum on the satellite was at a frequency of 1 Hz; at ground stations, the spectral maximum splits into 0.95 and 1.1 Hz. In interval B, the spectral maximum on the satellite is observed at 1.35 Hz; and on Earth, at 1.3 Hz. The frequency of oscillations, recorded at all ground stations, coincides with the frequency of oscillations on the satellite and does not change as they propagate to low latitudes. The relative half-widths of

the Pc1 pulsation spectrum $\Delta f/f_{max}$ (Δf is the width of the spectral peak at half of the spectral maximum) on Earth and on the satellite are 0.12 and 0.07 respectively. The narrow spectral width $\Delta f/f_{max}$~0.1 suggests that in terms of plasma physics Pc1 pulsations should be considered in the approximation of a monochromatic wave.

Consider the orientation of the polarization ellipse. Polarization is highly susceptible to noise and was stable only at YAK and MSR. Hodographs of magnetic field variations in the horizontal plane B_x B_y, filtered in the band 0.5–2 Hz, are shown for interval B. The horizontal plane polarization hodograph for the 10 s interval at ~14:20:20 UT is superimposed on the map with the orbit's position (Figure 8). The major axis of the polarization ellipses at these stations is seen to "looks at the epicenter" of Pc1 activity according to satellite data.

SPATIAL AND POLARIZATION STRUCTURE OF Pc1 WAVE PACKETS IN THE IONOSPHERE

To thoroughly define polarization and duration of the wave packet in the ionosphere, let us examine the magnetograms (B_x, B_y, B_z) of variations from SWARM C (filtered in the 0.1–5 Hz band) for interval A (Figure 9) and from SWARM B for interval B (Figure 10). In the MFA coordinate system, the field-aligned magnetic field component of the wave is practically absent B_z~0, i.e. the oscillations are indeed transverse. The oscillations are Alfvén wave packets incident on the ionosphere rather than FMS modes of the ionospheric waveguide. The most intense is the transverse radial component B_x. The peak-to-peak amplitude in this component is ~0.4 nT in interval A and ~1.8 nT in interval B. On Earth, the peak-to-peak amplitude of the most intense B_x component is ~15 nT in both events.

Thus, the amplitude of ground pulsations is almost two orders of magnitude lower than the wave amplitude in the ionosphere.

The filtered oscillations are a series of wave packets from the satellite and the ground observatory that do not match. For example, Figure 9 shows the delay in the ground response to a satellite wave packet Δt~10 s. At the beginning of interval A, the distance between YAK and the projection of the SWARM-C orbit onto the ionosphere is ~1350 km. At the beginning of interval B, the

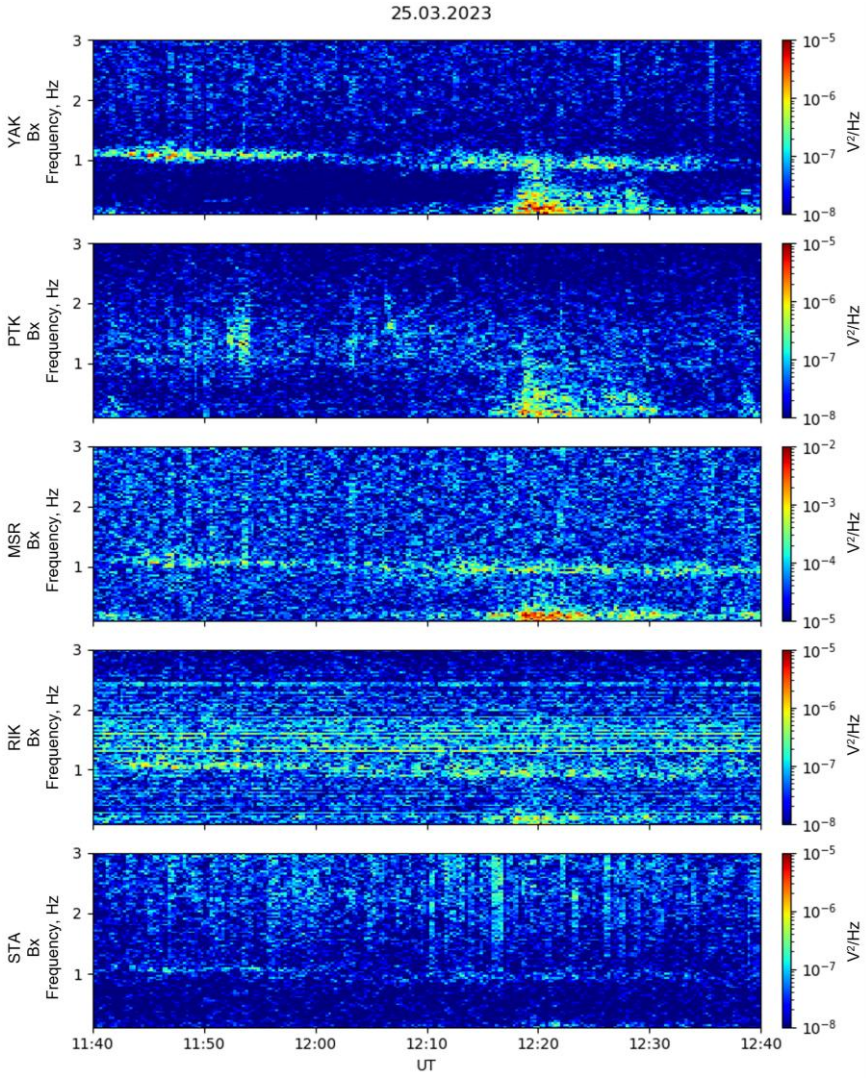

Figure 2. Spectrograms of the B_x components from a chain of stations given according to decreasing latitude (YAK, PTK, MSR, RIK, STA) for interval A (11:40–12:40 UT) on March 25, 2023

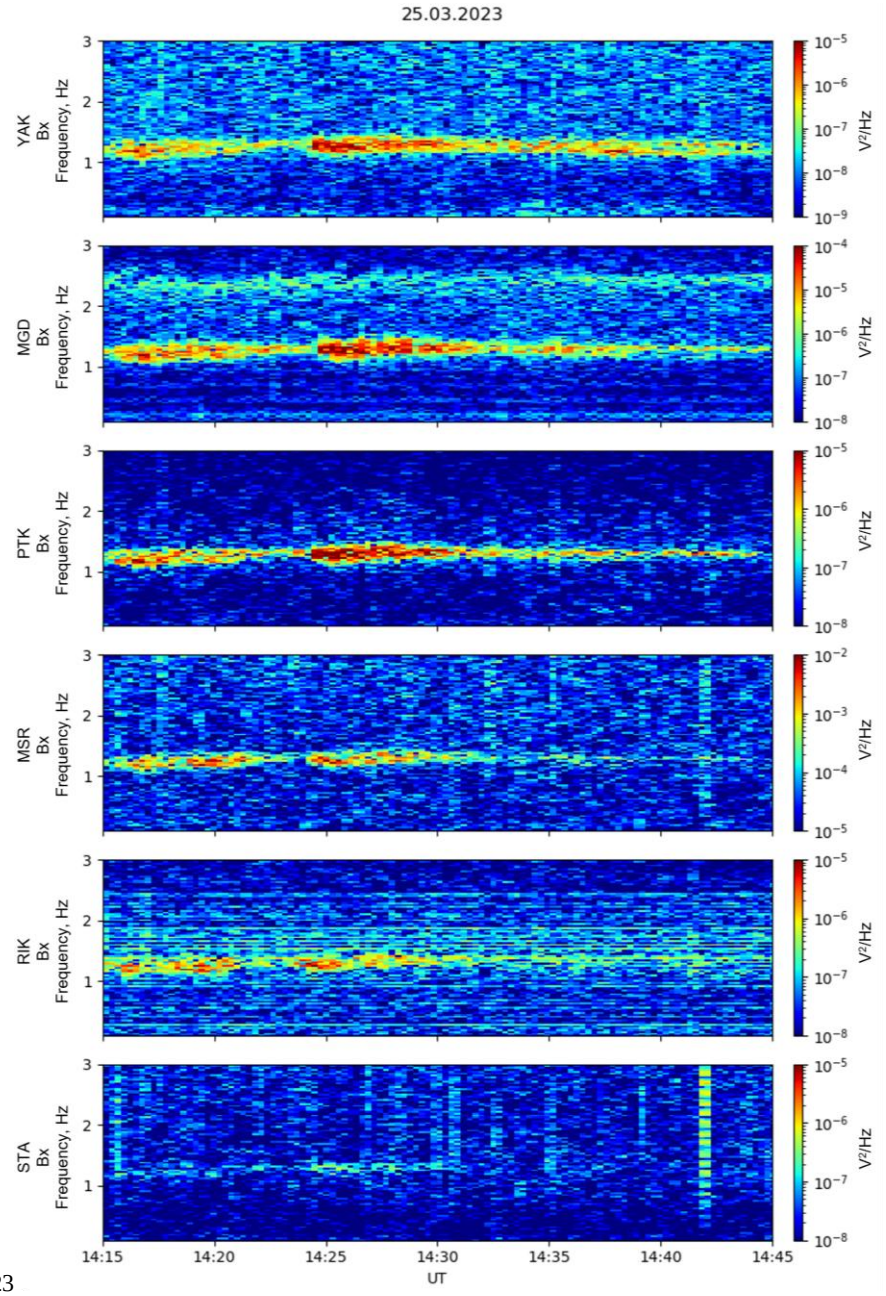

2023

Figure 3. Spectrograms of horizontal B_x from YAK, MGD, PTK, MSR, RIK, and STA for interval B (14:15–14:45 UT) on March 25, 2023

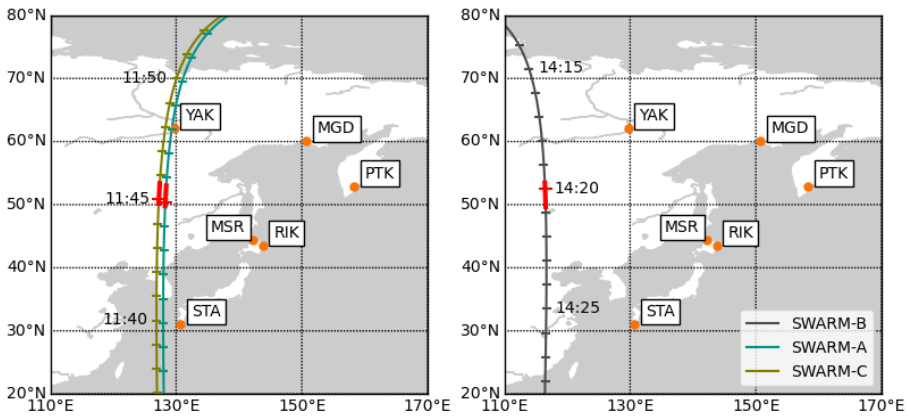

Figure 4. Map in geographic coordinates with the position of the stations and the geomagnetic projection of the orbit of each of the SWARM satellites along the field line onto the lower ionosphere (100 km) for intervals A (*a*) and B (*b*). The red color indicates the section of the orbit where Pc1 oscillations were recorded.

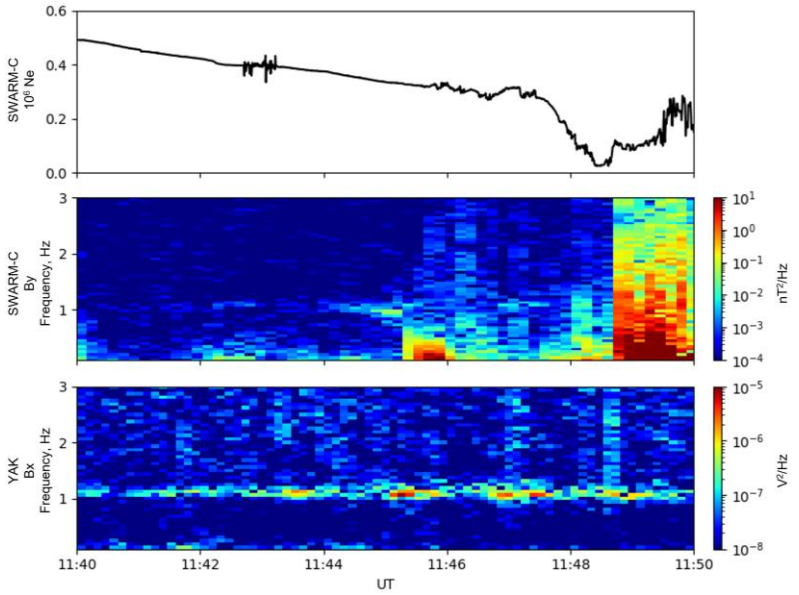

Figure 5. Variations in plasma density N_e for interval A according to data from the SWARM-C Langmuir probe (*a*); magnetic oscillation spectrogram (B_y) from SWARM C (*b*), and magnetic pulsation spectrogram (B_x) from YAK (*c*)

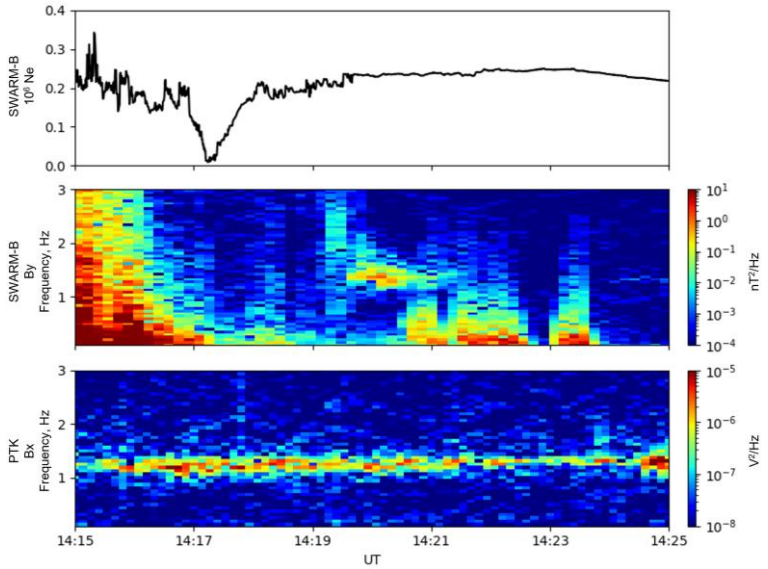

Figure 6. Variations in plasma density N_e for interval B according to data from the SWARM-B Langmuir probe (*a*); magnetic oscillation spectrogram from SWARM B (*b*), and magnetic pulsation spectrogram (B_x) from PTK (~~*b*~~*c*)

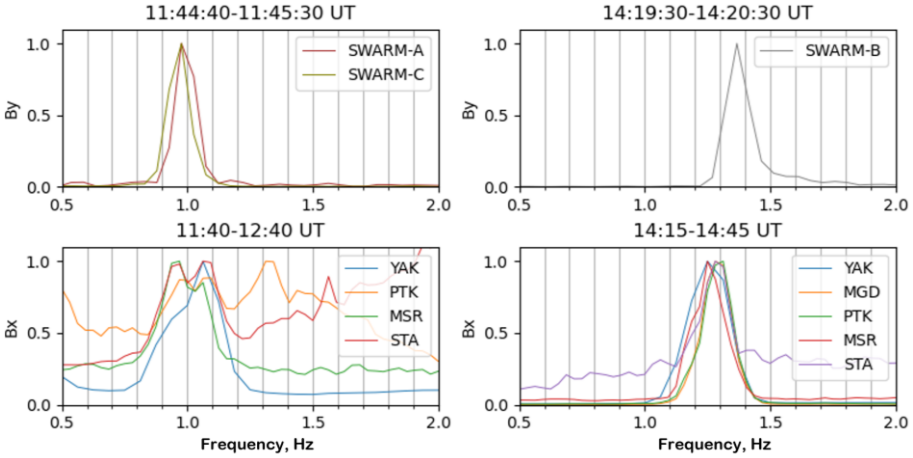

Figure 7. Normalized spectra of the B_x component of all stations separately for intervals A (*a*) and B (*b*) at frequencies 0.5–2.0 Hz~~.~~ At the top are signal spectra from respective satellites. The RIK station is excluded because high-frequency interference at it strongly distorts the spectrum.

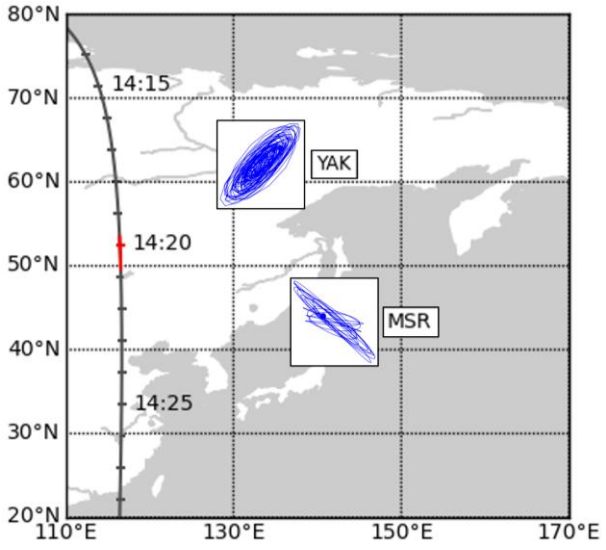

Figure 8. Hodographs of magnetic field variations for the 10 s interval at ~14:20:20 UT in the horizontal plane B_x B_y (signals filtered in the 0.5–2 Hz band), constructed for YAK and MSR

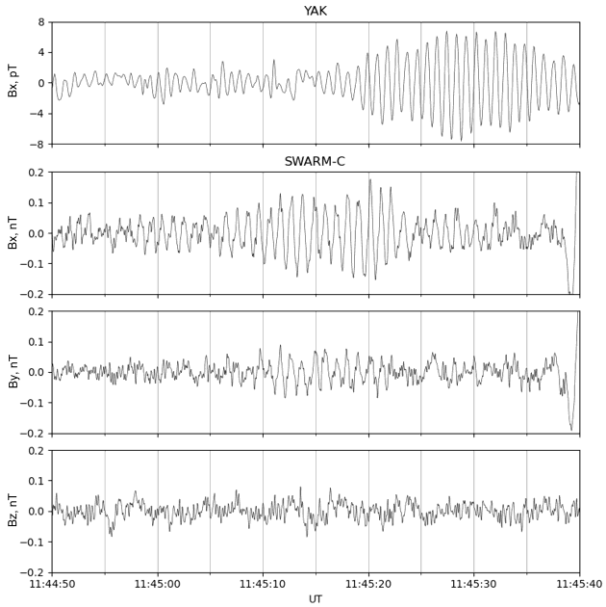

Figure 9. Magnetograms (B_x, B_y, B_z) of variations from SWARM C (filtered in the 0.1–5 Hz band) and magnetogram (B_x) from YAK for the time interval 11:44:50–11:45:40 UT

distance between PTK and the SWARM-B orbit projection is ~2790 km. The observed delay of ~10 s at ~1350 km distances to the site of wave incidence corresponds to propagation along the ionosphere with an apparent velocity of ~ 135 km/s. In order of magnitude, this estimate matches the typical values of the Alfvén velocity at the F-layer maximum of the dayside ionosphere.

The short burst of the intensity of Pc1 oscillations detected by the satellite can be attributed to the intersection of a localized region occupied by a wave packet. For interval A, the duration of the burst observed by SWARM C τ~25 s; and for interval B by SWARM B, τ~45 s. During this time, the satellites at a velocity V_s~7.5 km/s pass the distance $V_s\tau$~180 km and ~340 km respectively. This rough estimate can be taken as the transverse size of the wave packet. When projected onto the ionosphere at an altitude of 100 km, it is ~170 and ~320 km. Yet, using the data from one satellite it is impossible to determine whether the modulation of the packet amplitude is a consequence of fluctuations in the signal generator in a given flux tube or the intersection of several close flux tubes of different scales with various signal amplitudes. The presence of two close satellites suggests that when they are in the same flux tube, the coherence of the recorded signals is high; if one of them leaves the tube, the coherence decreases. For a more rigorous quantitative assessment of the spatial scale of the wave packet detected by SWARM A and C, we have obtained a dynamic squared wavelet coherence $\gamma^2(f)$ [https://pycwt.readthedocs.io/en/latest/] for interval A (Figure 11). According to [Grinsted et al., 2004], the wavelet coherence is found as

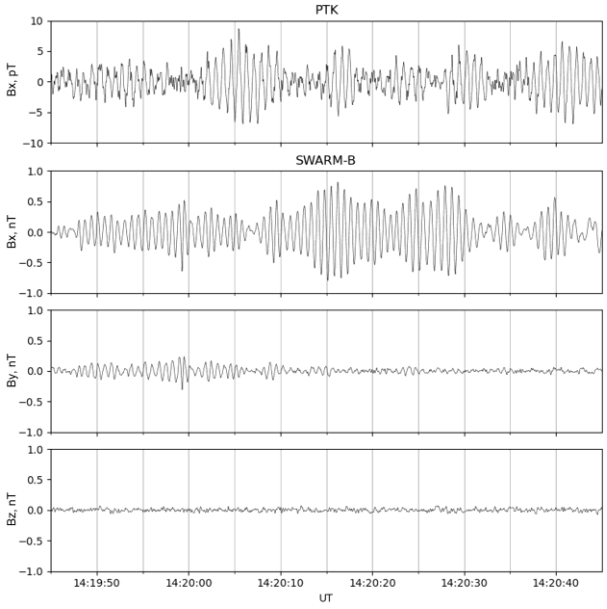

Figure 10. Magnetograms of oscillations from SWARM B (B_x, B_y, B_z) and magnetograms of pulsations (B_x) from PTK for the time interval 14:19:45–14:20:45 UT. The time series are filtered in the 0.1–5 Hz band

$$\gamma^2(t) = \frac{\left|S\left(t^{-1}W^{XY}(t)\right)\right|^2}{S\left(t^{-1}\left|W^X(t)\right|^2\right)S\left(t^{-1}\left|W^Y(t)\right|^2\right)},$$

where W^X, W^Y, $W^{XY}=W^X W^{Y*}$ are wavelets and cross-wavelets of signals X and Y; S is the smoothing operator; * is the complex conjugation. High coherence (γ^2>0.8) is observed only in the interval 11:45:04–11:45:16 UT, i.e. for 12 s. It is assumed that during this period both satellites are located inside a spatially limited wave packet. So, the transverse size of the flux tube occupied by the wave packet is ~90 km.

The phase cross-spectrum between the pulsations for SWARM A and C was also estimated using the Blackman—Tukey method (Figure 12). In the frequency domain with high coherence (γ^2~0.5) and high amplitude of autospectra, the phase shift $\Delta\varphi$~80°. From the fact that SWARM A flies further east than SWARM C, and

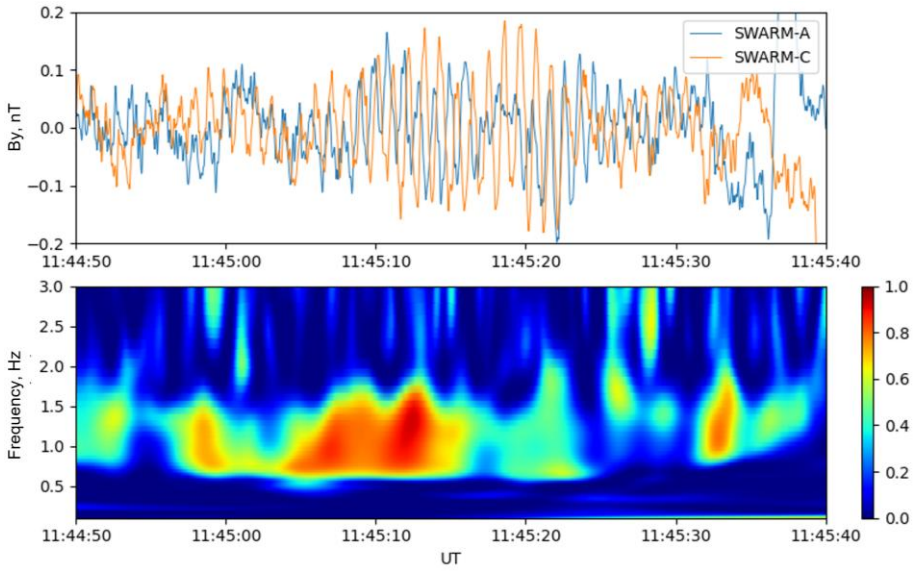

Figure 11. Dynamic wavelet coherence of Pc1 oscillations $\gamma^2(f)$ recorded by SWARM A and C for the interval 11:44:50–11:45:40 UT

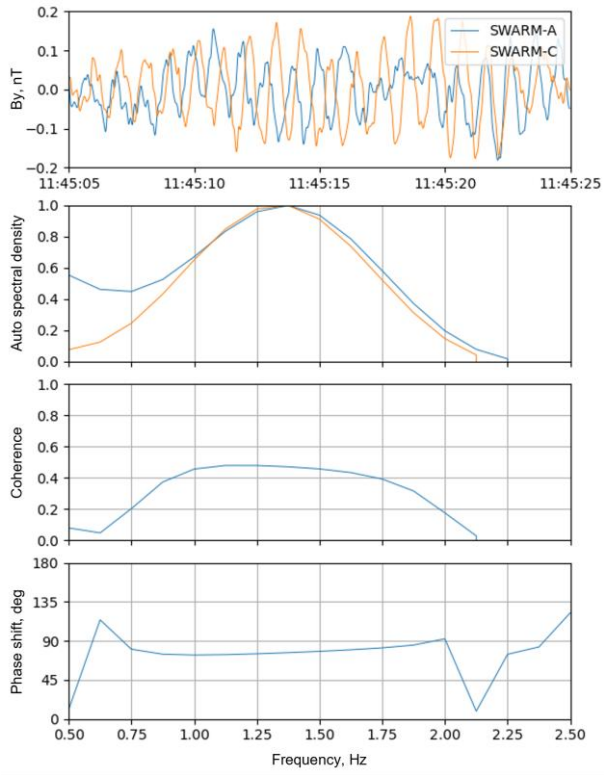

Figure 12. Phase cross-spectrum between pulsations on SWARM A and C, calculated using the Blackman—Tukey method

the signal on SWARM A is clearly ahead that on SWARM C (see Figure 12, *a*) it follows that the apparent phase velocity of the signal has an azimuthal westerly direction (i.e., the proton drift direction). The magnitude of the transverse wave vector can be estimated from the ratio $k_\perp \sim (\pi/180°)\Delta\varphi/\Delta x$, which, when the distance between the satellites is $\Delta x \sim 100$ km, yields $k_\perp \sim 4\cdot10^{-3}$ km^{-1}. The longitudinal wavenumber can be estimated from the ratio $k_\parallel \sim \omega/V_A \sim 6\cdot10^{-3}$ km^{-1} (at $V_A=10^3$ km/s). Thus, the selected phase shift indicates that the wavefront deviates significantly from field-aligned propagation $k_\perp \sim k_\parallel$.

DISCUSSION

One of the fundamental questions of magnetospheric physics is how well Pc1 ground observations characterize activity of EMIC waves in the magnetosphere [Guglielmi, Potapov, 2019]. It is important because Pc1 pulsations are considered responsible for pitch-angle scattering and precipitation of relativistic radiation belt electrons [Miyoshi et al., 2008] and energetic ring current protons [Kennel and Petchek, 1966; Yahnina et al., 2000] into the atmosphere, i.e. EMIC wave activity is one of the factors that control the dynamics of the radiation belt and the ring current.

Analysis of this event has shown that ground Pc1 pulsations are not just a "copy" of magnetospheric EMIC waves. A significant difference between the signals received by the satellite and ground stations is related to the effective propagation in the ionospheric waveguide. As it propagates, polarization of the ground geomagnetic response changes due to a change in the type of signal in the ionosphere. Near the source (at a distance from the point of incidence of the order of the transverse scale of the wave beam), the Alfvén mode such that the 2D vector $\mathrm{div}\mathbf{B}_\perp=0$ prevails in the signal structure. Thus, the signal should be polarized perpendicular to the propagation direction specified by the vector $\mathbf{k}_\perp$. At a distance from the source (i.e., at a distance of more than several scales of the wave beam), the waveguide FMS mode such that $\mathrm{rot}\mathbf{B}_\perp=0$ prevails. In this case, the signal should be polarized along $\mathbf{k}_\perp$, i.e. the major axis should face the source. The orientation of the polarization ellipse observed at the mid-latitude YAK and MSR stations (see Figure 8) confirms these ideas. At lower-latitude stations, the polarization ellipse becomes unstable.

Due to the presence of two close satellites, we managed to determine in detail the amplitude-phase structure of the wave packet in the ionosphere. The wave packet is limited in the transverse direction by a flux tube ~100 km in size. The phase front of the wave propagating inside the tube deviates significantly from field-aligned propagation along the geomagnetic field, $k_\perp \sim k_\parallel$. The theory of EMIC wave generation is based on the assumption of their quasi-longitudinal propagation in which the wave vector remains parallel to the external magnetic field $\mathbf{B}_0$ since it is precisely such waves that can effectively interact with resonant protons. However, in inhomogeneous plasma transverse inhomogeneity inevitably leads to a rapid growth of the transverse component of the wave vector $k_\perp$, i.e., to fragmentation of the transverse spatial structure of the packet [Guglielmi, 1970]. The transverse wave vector when passing along the field line for a distance S grows according to the law $\Delta k_\perp = \partial_x \omega_A(x)(S/V_A)$, where $\omega_A = k_\parallel V_A$. At the scale of the longitudinal inhomogeneity of the Alfvén velocity $a=R_E$, the Alfvén packet wavefront having traveled the distance along the field line $S>R_E$ becomes inclined — $|k_\perp/k_\parallel|>1$. Additional fragmentation of the transverse scale of the wave packet incident on the ionosphere along the geomagnetic field with inclination I, i.e. an increase in the wave vector transverse component, can occur upon reflection from the ionosphere by $\Delta k_\perp = 2\, k_\parallel \cot I$. This relation follows from Snell's law on the conservation of the horizontal component of the wave vector $\{k_{\perp x}\}=0$. An increase in $k_\perp$ should remove the wave packet from resonance with energetic protons since EMIC instability effectively enhances only quasi-longitudinally propagating waves for which $k_\perp < k_\perp^*$. The critical transverse scale is determined by the value $k_\perp^* = k_\parallel \left(\omega/\Omega_i\right)$ [Leonovich, 1984]. Therefore, as the packet propagates, it should become quasi-transverse, and its enhancement is impossible. It is only under special conditions in the region with a sharp plasma gradient (plasmapause) that the plasma and magnetic field irregularities can partially balance each other and the multiple enhancement mode becomes possible when a wave passes through the near-equatorial region of the magnetosphere [Dmitrienko, Mazur, 1992]. However, in the real magnetosphere the radial plasma structure is quite rugged which can give rise to local waveguides for EMIC waves due to the combined action of the transverse wave dispersion and the nonmonotonic distribution of V_A across $\mathbf{B}_0$. Waveguide propagation is possible only in the vicinity of the top of the field line, where the finite frequency ratio ω/Ω_i, which defines the transverse dispersion, is finite. In the event considered, as well as in the events described in the literature, the ratio between the Pc1 transverse and longitudinal scales of the wave packet $|k_\perp/k_\parallel|>1$, i.e. the quasi-transverse propagation mode is rather realized. The available theoretical models of longitudinal waveguide propagation of EMIC waves [Leonovich et al., 1983] do not yet provide an explanation for the mechanism of formation of the localized transverse structure of Pc1 waves. The question of how the transverse scale of EMIC waves in the magnetosphere is determined remains open. It is possible that the quasi-longitudinal propagation mode is implemented in the vicinity of the top of the field line, but as it approaches the ionosphere, refraction makes the wavefront inclined. The adoption of such a mechanism makes the possibility of effective reflection of the wave from the ionosphere and its return to the generation region doubtful.

One of the fundamental problems in studying the spatial structure of wave disturbances in near-Earth plasma is related to the inability to separate spatial and temporal variations in single-satellite observations. Observations on magnetospheric satellites provide much information about temporal evolution of Pc1 waves in the near-equatorial region of the magnetosphere, but it is impossible to identify the transverse spatial structure of the waves from them. Due to the possibility of long-range (up to a thousand kilometers) propagation of Pc1 signals in the ionospheric FMS waveguide, ground observations also cannot be used to determine the transverse structure of EMIC waves incident on the ionosphere. Based on indirect data, Erlandson et al. [1990] attributed the short duration (<5 min) of Pc1 wave bursts, recorded on the Viking satellite, to small-scale wave structure, which was 40–150 km in projection onto the ionosphere. EMIC waves on the Arase and RBSP satellites were observed in a narrow region of L shells ~185 km in size in the ionosphere [Matsuda et al., 2021]. Precipitation of energetic (>30 keV) protons caused by scattering by EMIC waves [Yahnina et al., 2008] and subauroral aurorae [Yahnin et al., 2007; Sakaguchi et al., 2008] are also limited in latitude $\Delta\Phi \sim 1.0°$. During the ST5 experiment, three low-orbit microsatellites were placed into the same orbit, forming a configuration of pearls on a string, and crossed the same region of space with a delay ~1–10 min [Engebretson et al., 2008]. Analysis of Pc1 wave packets recorded during ST5 allowed us to separate spatial and temporal structures of EMIC waves and showed their narrow localization in latitude with characteristic scales from the first tens to hundreds of kilometers [Pilipenko et al., 2012]. Thus, estimated scale of Pc1 waves from the pair of SWARM satellites is consistent with the available fragmentary information from other observations in the upper ionosphere.

In the event considered, synchronous satellite and ground observations confirmed that while long-term pulsations are observed at ground stations, only short bursts of Pc1 pulsations are recorded by ionospheric satellites. It is natural to assume that the generation region in the magnetosphere is very local and a wave packet is detected only when a satellite directly crosses the flux tube filled with EMIC pulsations, whereas a ground station collects signals from a large area. Yet, this explanation is not sufficient to interpret ST5 observations, where out of several dozen recorded Pc1 packets in no case was the signal consistently observed by all three satellites [Engebretson et al., 2008]. The EMIC instability is likely to develop in the near-equatorial magnetosphere with an intense ring current not in the continuous pulsation mode, but in the form of a series of relatively short (<10 min) highly localized irregular bursts

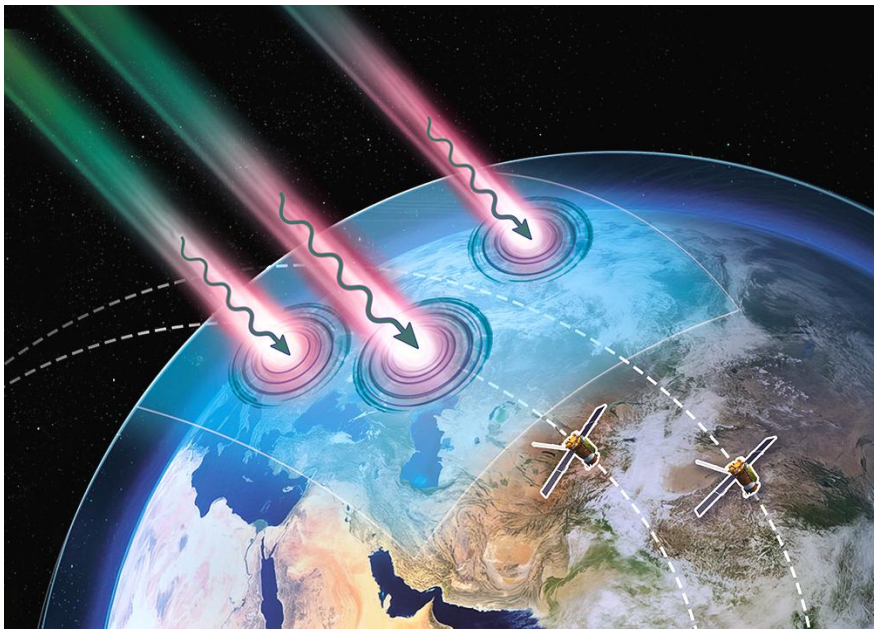

Figure 13. Qualitative illustration of the proposed mode of excitation of localized bursts of Pc1 wave packets and their propagation to ground stations

of instability, chaotically distributed in a finite region of space, where there are intense energetic proton fluxes. The region of occurrence of Pc1 pulsations in longitude covers, on average, an interval of ~82° and is determined by the scale of unstable energetic proton fluxes rather than by ionospheric propagation [Liu et al., 2023]. Qualitatively, this mode of excitation and propagation of Pc1 pulsations is shown in Figure 13. The hypothesis requires a more rigorous theoretical justification and experimental verification.

It seems to us that the EMIC instability of ring current protons primarily works not as a convective amplifier of bouncing wave packets, but as a generator of wave bursts. Indeed, as the thermal plasma pressure increases, the group velocity of EMIC waves decreases, which can lead to the transition of the instability from convective to absolute. According to theoretical estimates, such a transition occurs at $\beta_\perp \left(T_\perp / T_\parallel\right)^2 \geq 3.5$, where $\beta_\perp$ is the ratio of the transverse thermal plasma pressure to the magnetic pressure [Wandzura, Coroniti, 1975]. This condition may well be fulfilled for ring current protons near the top of the field line even during the magnetic storm recovery phase. The presence of finite β in the generation region of EMIC waves can be indicated by a diamagnetic decrease in the magnetospheric magnetic field [Yin et al., 2024]. The increment of kinetic EMIC instability is small, and in one pass from the generation region to the upper ionosphere the wave does not have time to gain sufficient energy. Therefore, EMIC instability is most likely to be excited not in the soft mode, but in the hard self-excitation mode [Guglielmi, 2015]. In the meantime, the physical causes of many characteristic properties of Pc1 pulsations remain unclear: under what conditions does convective or absolute EMIC instability develop? What determines the transverse size of the generated wave packets? Why is there no long-term pulsation generation in the same flux tube?

When studying the dynamics of Earth's radiation belt, it is believed that Pc1 EMIC waves can cause relativistic electrons to precipitate from the outer radiation belt into the atmosphere and thus reduce the level of "killer electron" fluxes to a safe level for satellite electronics [Miyoshi et al., 2008]. It follows from the resonant condition that a wave packet traveling to the ionosphere during interaction scatters particles (energetic protons or relativistic electrons), which go into the conjugate ionosphere, into the loss cone. It, however, remains unclear whether precipitation of relativistic electrons under the action of EMIC wave with small transverse scales (<100 km in the projection onto the ionosphere) can affect the overall electron balance of the radiation belt.

CONCLUSION

The event considered — excitation of Pc1 pulsations during the recovery phase of the March 25, 2023 magnetic storm — is a fairly typical phenomenon for which a unique set of satellite and ground data has been collected. An attempt to explain the set of the observed properties of Pc1 pulsations necessitated to express a number of hypotheses about mechanisms of generation of these waves. Presumably, EMIC instability develops in the "popcorn in a hot pan" regime as a long series of localized bursts of generation lasting less than 10 min (see Figure 13). In this case, each burst of instability develops in another nearby flux tube. A low-orbit satellite can detect only a short burst of EMIC pulsations when flying directly through the generation region. A ground station that collects ionospheric responses from a large area records a long continuous series of oscillations. Nonetheless, these assumptions have not yet been supported by any theoretical modeling.

The work was financially supported by RSF Grant No. 24-77-10012. We thank O.S. Mikhailova for helpful advice, K. Shiokawa, the head of the PWING project, I.N. Poddelsky, the head of the Magadan Observatory, for the data provided, and the reviewers for their useful comments.

REFERENCES

Anderson B.J., Erlandson R.E., Zanetti L.J. A statistical study of Pc1-2 magnetic pulsations in the equatorial magnetosphere: 1. Equatorial occurrence distributions. *J. Geophys. Res.* 1992, vol. 97, pp. 3075–3088. DOI: 10.1029/91ja02697.

Arcimovich L.A., Sagdeev R.Z. *Fizika plazmy dlya fizikov* [Physics plasma for physicists]. Moscow, Atomizdat Publ., 1979, 313 p. (In Russian).

Demekhov A.G. Recent progress in understanding Pc1 pearl formation. *J. Atmos. Solar-Terr. Phys*. 2007, vol. 69, no. 14, pp. 1609–1622. DOI: 10.1016/j.jastp.2007.01.014.

Dmitrienko I.S., Mazur V.A. The spatial structure of quasicircular Alfven modes of waveguide at the plasmapause — Interpretation of Pc1 pulsations. *Planet. Space Sci*. 1992, vol. 40, iss. 1, pp. 139–148. DOI: 10.1016/0032-0633(92)90156-i.

Engebretson M.J., Peterson W.K., Posch J.L., Klatt M.R., Anderson B.J., Russell C.T., et al. Observations of two types of Pc1-2 pulsations in the outer dayside magnetosphere. *J. Geophys. Res*. 2002, vol. 107, iss. A12, p. 1451. DOI: 10.1029/2001JA000198.

Engebretson M.J., Posch J.L., Westerman A.M., Otto N.J., Slavin J.A., Le G., et al. Temporal and spatial characteristics of Pc1 waves observed by ST5. *J. Geophys. Res.* 2008, vol. 113, A07206. DOI: 10.1029/2008JA013145.

Erlandson R.E., Zanetti L.J., Potemra T.A., Block L.P., Holmgren G. Viking magnetic and electric field observations of Pc1 waves at high latitudes. *J. Geophys. Res*. 1990, vol. 95, iss. A5, pp. 5941–5955. DOI: 10.1029/ja095ia05p05941.

Fedorov E.N., Pilipenko V.A., Engebretson M.J., Hartinger M.D. Transmission of a magnetospheric Pc1 wave beam through the ionosphere to the ground. *J. Geophys. Res*. 2018, vol. 123, iss. 5, pp. 3965–3982. DOI: 10.1029/2018JA 0253381–18.

Fujita S., Tamao T. Duct propagation of hydromagnetic waves in the upper ionosphere. 1. Electromagnetic field disturbances in high latitudes associated with localized incidence of a shear Alfven wave. *J. Geophys. Res.* 1988, vol. 93, iss. A12, pp. 14665–14673. DOI: 10.1029/ja093ia12p14665.

Gary S.P., Thomsen M.F., Yin L., Winske D. Electromagnetic proton cyclotron instability: Interactions with magnetospheric protons. *J. Geophys. Res.* 1995, vol. 100, no. A11, pp. 21961–21972. DOI: 10.1029/95ja01403.

Grinsted A., Moore J.C., Jevrejeva S. Application of cross wavelet transform and wavelet coherence to geophysical time series. *Nonlinear Processes in Geophysics*. 2004, vol. 11, no. 5/6, pp. 561–566. DOI: 10.5194/npg-11-561-2004.

Guglielmi A.V. Cyclotron instability in the magnetosphere considering the refraction of rising waves. *Geomagnetism and Aeronomy*. 1970, vol. 10, no. 4, pp. 721–724.

Guglielmi A.V. *MGD-volny v okolozemnoj plazme* [MHD waves in near-Earth plasma]. Moscow, Nauka Publ., 1979, 139 p. (In Russian).

Guglielmi A.V. Three unsolved problems in the physics of magnetospheric waves Pc1. *Geofizicheskie Issledovanija* [Geophysical Research], 2015, vol. 16, no. 3, pp. 63–72. (In Russian).

Guglielmi A.V., Potapov A.S. Problems of the Pc1 magnetospheric wave theory. A review. *Solar-Terr. Phys*. 2019, vol. 5, iss. 3, pp. 87–92. DOI: 10.12737/stp-53201910.

Guglielmi A.V., Potapov A.S., Russell C.T. The ion cyclotron resonator in the magnetosphere. *JETP Lett*. 2000, vol. 72, no. 6, pp. 298–300. DOI: 10.1134/1.1328441.

Hansen H.J., Fraser B.J., Menk F.W., Hu Y.-D., Newell P.T., Meng C.-I., Morris R.J. High-latitude Pc 1 bursts arising in the dayside boundary layer region. *J. Geophys. Res*. 1992, vol. 97, no. A4, pp. 3993–4008. DOI: 10.1029/91ja01456.

Horne R.B., Thorne R.M. On the preferred source location for the convective amplification of ion cyclotron waves. *J. Geophys. Res.* 1993, vol. 98, no. A6, pp. 9233–9248. DOI: 10.1029/92ja02972.

Horne R.B., Thorne R.M. Convective instabilities of electromagnetic ion cyclotron waves in the outer magnetosphere. *J. Geophys. Res*. 1994, vol. 99, no. A9, pp. 17259–17273. DOI: 10.1029/94ja01259.

Hu Y.D., Fraser B.J. Electromagnetic ion cyclotron wave amplification and source regions in the magnetosphere. *J. Geophys. Res*. 1994, vol. 99, no. A1, pp. 263–272. DOI: 10.1029/93ja01897.

Johnson J.R., Cheng C.Z. Can ion cyclotron waves propagate to the ground? *Geophys. Res. Lett*. 1999, vol. 26, no. 6, pp. 671–674. DOI: 10.1029/1999gl900074.

Kangas J., Guglielmi A., Pokhotelov O. Morphology and physics of short-period geomagnetic pulsations. *Space. Sci. Rev.* 1998, vol. 83, no. 3/4, pp. 435–512. DOI: 10.1023/A:1005063911643.

Keika K., Takahashi K., Ukhorskiy A.Y., Miyoshi Y. Global characteristics of electromagnetic ion cyclotron waves: Occurrence rate and its storm dependence, *J. Geophys. Res*. 2013, vol. 118, no. 7, pp. 4135–4150, DOI: 10.1002/jgra.50385.

Kennel C.F., Petchek H.E. Limit on stably trapped particle fluxes. *J. Geophys. Res*. 1966, vol. 71, no. 1, pp. 1–28. DOI: 10.1029/jz071i001p00001.

Kim H., Lessard M.R., Engebretson M.J., Lühr H. Ducting characteristics of Pc1 waves at high latitudes on the ground and in space. *J. Geophys. Res*. 2010, vol. 115, A09310. DOI: 10.1029/2010JA015323.

Leonovich A.S. Propagation of geomagnetic pulsations in magnetospheric ducts. *Geomagnetism and Aeronomy*. 1984, vol. 24, no. 1, p. 94.

Leonovich A.S., Mazur V.A., Senatorov V.N An Alfven waveguide. *J. Experimental and Theoretical Phys.* 1983, vol. 85, pp. 141–145. (In Russian).

Liu J., Shiokawa K., Oyama S.-I., Otsuka, Y., Jun, C.-W., Nosé, M., et al. A statistical study of longitudinal extent of Pc1 pulsations using seven PWING ground stations at subauroral latitudes. *J. Geophys. Res*. 2023, vol. 128, no. 1, 2021JA029987. DOI: 10.1029/2021JA029987.

Matsuda S., Miyoshi Y., Kasahara Y., Blum L., Colpitts C., Asamura K., et al. Multipoint measurement of fine-structured EMIC waves by Arase, Van Allen Probe A, and ground stations. *Geophys. Res. Lett.* 2021, vol. 48, e2021GL096488. DOI: 10.1029/2021GL096488.

Mikhailova O.S., Klimushkin D.Yu., Mager P.N. Pc1-pulsations: the parallel structure in the magnetosphere plasma with admixture of the heavy ions. *Adv. Astron. Space Phys*. 2012, vol. 2, pp. 88–90.

Mikhailova O.S. The spatial structure of ULF waves in the equatorial resonator localized at the plasmapause with the admixture of the heavy ions. *J. Atmos. Solar-Terr. Phys*. 2014, vol. 108, pp. 10–16. DOI: 10.1016/j.jastp.2013.12.007.

Mikhailova O.S., Klimushkin D.Yu., Mager P.N. The current state of the theory of Pc1 range ULF pulsations in magnetospheric plasma with heavy ions: A review. *Solar-Terr. Phys*. 2022, vol. 8, iss. 1, pp. 3–18. DOI: 10.12737/stp-81202201.

Miyoshi Y., Sakaguchi K., Shiokawa K., Evans D., Albert J., Connors M., Jordanova V. Precipitation of radiation belt electrons by EMIC waves, observed from ground and space. *Geophys. Res. Lett.* 2008, vol. 35, L23101. DOI: 10.1029/2008GL035727.

Mursula K. Satellite observations of Pc1 pearl waves: The changing paradigm. *J. Atmos. Solar-Terr. Phys.* 2007, vol. 69, pp. 1623–1634. DOI: 10.1016/j.jastp.2007.02.013.

Pilipenko V.A., Polozova T.L., Engebretson M. Space-time structure of ion-cyclotron waves in the topside ionosphere as observed onboard the ST-5 satellites. *Cosmic. Res*. 2012, vol. 50, no. 5, pp. 329–329. DOI: 10.1134/S001095251 2050048.

Rauch J.L., Roux A. Ray tracing of ULF waves in a multicomponent magnetospheric plasma: consequences for the generation mechanism of ion cyclotron waves. *J. Geophys. Res.* 1982, vol. 87, no. A10, pp. 8191–8198. DOI: 10.1029/JA087iA10p08191.

Sakaguchi K., Shiokawa K., Miyoshi Y., Otsuka Y., Ogawa T., Asamura K., Connors M. Simultaneous appearance of isolated auroral arcs and Pc1 geomagnetic pulsations at subauroral latitudes. *J. Geophys. Res*. 2008, vol. 113, A05201. DOI: 10.1029/2007JA012888.

Shiokawa K., Katoh Y., Hamaguchi Y., Yamamoto Y., Adachi T., Ozaki M., et al. Ground-based instruments of the PWING project to investigate dynamics of the inner magnetosphere at subauroral latitudes as a part of the ERG-ground coordinated observation network. *Earth, Planets and Space*. 2017, vol. 69, no. 1, article number 160. DOI: 10.1186/s40623-017-0745-9.

Trakhtengerts V.Y., Demekhov A.C. Generation of Pc1 pulsations in the regime of backward wave oscillator. *J. Atmos. Solar-Terr. Phys*. 2007, vol. 69, pp. 1651–1656. DOI: 10.1016/j.jastp.2007.02.009.

Trakhtengerts V.Y., Rycroft M.J. *Whistler and Alfvén mode cyclotron masers in space*. Cambridge University Press, 2011, 354 p.

Usanova M.E., Mann I.R., Rae I.J., Kale Z.C., Angelopoulos V., Bonnell J.W., et al. Multipoint observations of magnetospheric compression-related EMIC Pc1 waves by THEMIS and CARISMA. *Geophys. Res. Lett*. 2008, vol. 35, L17S25. DOI: 10.1029/2008GL034458.

Wandzura S., Coroniti F.V. Nonconvective ion cyclotron instability. *Planet. Space Sci*. 1975, vol. 23, pp. 123–131. DOI: 10.1016/0032-0633(75)90073-2.

Yahnina T.A., Frey H.U., Bösinger T., Yahnin A.G. Evidence for subauroral proton flashes on the dayside as the result of the ion cyclotron interaction. *J. Geophys. Res.* 2008, vol. 113, A07209. DOI: 10.1029/2008JA013099.

Yahnina T.A., Yahnin A.G., Kangas J., Manninen J. Proton precipitation related to Pcl pulsations. *Geophys. Res. Lett.* 2000, vol. 27, no. 21, pp. 3575–3578. DOI: 10.1029/2000gl003763.

Yahnin A.G., Yahnina T.A., Frey H.U. Subauroral proton spots visualize the Pc1 source. *J. Geophys. Res.* 2007, vol. 112, A10223. DOI: 10.1029/2007JA012501.

Yin Z.-F., Zhou X.-Z., Hu Z.-J., Yue C., Zong Q.G., Liu Z.Y., et al. Westward excursion of Pc1/EMIC waves and their source protons: Paradoxical observations from ground and space. *J. Geophys. Res.* 2024, vol. 129, e2023JA032317. DOI: 10.1029/e2023JA032317.

URL: https://stdb2.isee.nagoya-u.ac.jp/magne/magne_stations.html (accessed March 20, 2025).

URL: https://www.esa.int/Applications/Observing_the_Earth/FutureEO/Swarm (accessed March 20, 2025).

URL: https://sscweb.gsfc.nasa.gov (accessed March 20, 2025).

URL: https://pycwt.readthedocs.io/en/latest/ (accessed March 20, 2025).

Original Russian version: Pozdnyakova D.D., Pilipenko V.A., Nose M., Khomutov S.Yu., Baishev D.G., published in Solnechno-zemnaya fizika. 2025, vol. 11, no. 2, pp. 56–68. DOI: 10.12737/szf-112202505.

How to cite this article

Pozdnyakova D.D., Pilipenko V.A., Nose M., Khomutov S.Yu., Baishev D.G. Satellite and ground-based observations of Pc1 pulsations during a magnetic storm in March 2023. *Sol.-Terr. Phys*. 2025, vol. 11, iss. 2, pp. 48–59. DOI: 10.12737/stp-112202505.